

On the Anisotropy of Galactic Cosmic Rays

R. Schlickeiser^{1,2}, J. Oppotsch¹, M. Zhang³, and N. V. Pogorelov⁴

Institut für Theoretische Physik, Lehrstuhl IV: Weltraum- und Astrophysik, Ruhr-Universität Bochum D-44780 Bochum, Germany; rsch@tp4.rub.de, jo@tp4.rub.de
 Institut für Theoretische Physik und Astrophysik, Christian-Albrechts-Universität zu Kiel, Leibnizstr. 15, D-24118 Kiel, Germany
 Department of Physics and Space Sciences, Florida Institute of Technology, 150 W. University Boulevard, Melbourne, FL 32901, USA; mzhang@fit.edu
 Department of Space Science and Center for Space Plasma and Aeronomic Research, University of Alabama in Huntsville, 320 Sparkman Dr., Huntsville, AL

35899, USA; nikolai.pogorelov@uah.edu

Received 2019 April 1; revised 2019 May 23; accepted 2019 May 23; published 2019 July 1

Abstract

In the interstellar medium at rest, containing low-frequency magnetohydrodynamic linearly polarized slab Alfvén waves, the anisotropy of relativistic galactic cosmic rays consists of two parts: the streaming anisotropy $g_s(z, p, \mu)$, caused by the spatial gradient of the isotropic part of the cosmic ray distribution function, and the interstellar Compton–Getting anisotropy $g_c(z, p, \mu)$, caused by the momentum gradient of the isotropic part of the cosmic ray distribution function. Both anisotropies depend differently on the cosmic ray pitch-angle cosine μ , cosmic ray momentum p, and cross-helicity state H_c of the Alfvenic slab turbulence. First, the streaming anisotropy is independent from H_c and varies as $g_s(z, p, \mu) \propto (p|\mu|)^{\eta} \operatorname{sgn}(\mu)$ with $\eta = 2 - s$, where s denotes the power-law spectral index of interstellar turbulence. Second, the interstellar Compton–Getting anisotropy $g_c(z, p, \mu) \propto H_c \mu$ is independent of momentum and linearly proportional to $H_c \mu$. These different pitch-angle dependencies can be tested by the Liouville mapping technique to infer the pristine interstellar cosmic ray anisotropy from measurements inside the solar system. For cosmic rays with energy of 4 TeV the derived pristine interstellar cosmic ray anisotropy suggest the linear $(g \propto |\mu| \operatorname{sgn}(\mu))$ pitch-angle dependence. This is well explained by the interstellar Compton–Getting anisotropy, provided the Alfvén speed in the local interstellar medium is about $62 \operatorname{km s}^{-1}$.

Key words: cosmic rays - diffusion - ISM: magnetic fields - turbulence

1. Introduction

Observations of relativistic galactic cosmic rays indicate that their phase space distribution functions are nearly isotropic up to very high particle momenta (Ahlers & Mertsch 2017; Erlykin et al. 2019). In magnetized space plasmas this is readily explained by the presence of low-frequency linear ($\delta B \ll B_0$) transverse MHD waves (such as shear Alfvén and magnetosonic plasma waves). These transverse MHD waves have highly subluminal phase and group speeds $V_{\rm ph}=V_{\rm g}\leqslant V_{\rm A}\ll c$ less or equal to the Alfvén speed $V_A = 2.18 \cdot 10^5 B(\mu \text{G}) n_e^{-1/2} (\text{cm}^{-3})$ ${\rm cm\,s}^{-1}$, where c denotes the speed of light. Faraday's induction law then indicates for MHD waves that the strength of turbulent electric fields $\delta E = (V_A/c)\delta B \ll \delta B$ is much smaller than the strength of turbulent magnetic fields. Rapid gyromotion in the dominating uniform magnetic field B_0 establishes gyrotropic particle distribution functions for all charged particles independent from the gyrophase ϕ . On a slower but still fast timescale the turbulent magnetic fields δB , dominating over the turbulent electric fields δE , then by rapid pitch-angle scatterings generate nearly isotropic particle distribution functions independent from the pitch-angle cosine μ . Hence, the ordering $B_0 \gg \delta B \gg \delta E$ corresponds to the establishment of cosmic ray transport equations for

$$\langle f \rangle(\mathbf{x}, p, \mu, \phi, t) \rightarrow f_0(\mathbf{x}, p, \mu, t) \rightarrow F(\mathbf{x}, p, t),$$
 (1)

from the collision-free Boltzmann equation for the full phase space distribution $\langle f \rangle(\mathbf{x}, p, \mu, \phi, t)$, to the Fokker–Planck equation for its gyrotropic part $f_0(\mathbf{x}, p, \mu, t)$, and to the diffusion-convection transport equation for its isotropic part $F(\mathbf{x}, p, t)$, respectively (see, e.g., Schlickeiser 2002, 2011; Casanova & Schlickeiser 2012).

Accordingly, the cosmic ray anisotropy, defined as the deviation

$$g(\mathbf{x}, p, \mu, t) = f_0(\mathbf{x}, p, \mu, t) - F(\mathbf{x}, p, t)$$
 (2)

then is small $|g| \ll F$. The diffusion approximation (Jokipii 1966; Hasselmann & Wibberenz 1968; Earl 1974) applied to the Fokker–Planck transport equation for $f_0(\mathbf{x}, p, \mu, t)$ allows us to relate the cosmic ray anisotropy g to the solutions of the diffusion-convection transport equation for F.

We orient the large-scale guide magnetic field, which is uniform on the scales of the cosmic ray particles gyroradii $R_L = v/|\Omega_a|$, $B_0 = B_0 e_z = (0, 0, B_0)$ along the z-axis. v and $\Omega_a = q_a B_0/\gamma m_a c$ denote the speed and the relativistic gyrofrequency of a cosmic ray particle with mass m_a , charge q_a , energy $\gamma m_a c^2$, and momentum $p = \gamma m_a v$.

In the interstellar medium at rest containing slab Alfvén waves only, the Larmor-phase averaged steady-state Fokker–Planck transport equation is given by (Schlickeiser 1989)

$$v\mu \frac{\partial f_0}{\partial z} + \mathcal{R}f_0 - S(\mathbf{x}, p, t) = \frac{\partial}{\partial \mu} \left[D_{\mu\mu} \frac{\partial f_0}{\partial \mu} + D_{\mu p} \frac{\partial f_0}{\partial p} \right] + p^{-2} \frac{\partial}{\partial p} p^2 \left[D_{\mu p} \frac{\partial f_0}{\partial \mu} + D_{pp} \frac{\partial f_0}{\partial p} \right], \tag{3}$$

irrespective of how the Fokker–Planck coefficients are calculated, either by quasilinear (Schlickeiser 2002) or nonlinear (Shalchi 2009) cosmic ray transport theories. As the observed level of Alfvén wave intensities in the local interstellar medium is small compared to the strength of the uniform magnetic field, the quasilinear transport theory should well apply. S(x, p, t) denotes

the injection rate of cosmic rays, and

$$\mathcal{R}f = -p^{-2}\frac{\partial}{\partial p}[p^2\dot{p}_{\rm loss}f] + \frac{f}{T_c} \tag{4}$$

accounts for continuous $(\dot{p}_{\rm loss})$ and catastrophic (T_c) momentum losses of cosmic ray particles. We emphasize that in slab MHD turbulence (only Alfvén waves propagating parallel or antiparallel to the uniform guide magnetic field) $D_{\mu\mu}$, $D_{\mu p}$ and D_{pp} are the only nonvanishing Fokker–Planck coefficients.

2. Diffusion Approximation and Anisotropy

In the presence of low-frequency MHD plasma waves the pitch-angle Fokker–Planck coefficient $D_{\mu\mu}$ for energetic particles with $v\gg V_{\rm A}$ is the largest. Then the gyrotropic particle distribution function $f_0(x,p,\mu)$ under the action of low-frequency magnetohydrodynamic waves adjusts very quickly to a distribution function through pitch-angle diffusion, which is close to the isotropic distribution

$$F(\mathbf{x}, p) \equiv \frac{1}{2} \int_{-1}^{1} d\mu \, f_0(\mathbf{x}, p, \mu), \tag{5}$$

in the rest frame of the moving background plasma. Because of Equation (5) the cosmic ray anisotropy, defined in Equation (2) as the difference between the gyrotropic distribution function $f_0(x, p, \mu)$ and its isotropic part F(x, p), obeys

$$\int_{-1}^{1} d\mu \ g(\mathbf{x}, p, \mu) = 0. \tag{6}$$

In the Appendix it is shown that in the limit of the diffusion approximation $(|g| \ll F)$ the cosmic ray anisotropy consists of two parts

$$g(\mathbf{x}, p, \mu) \simeq g_{s}(\mathbf{x}, p, \mu) + g_{c}(\mathbf{x}, p, \mu),$$

$$g_{s}(\mathbf{x}, p, \mu) = -\frac{v}{4} \frac{\partial F(\mathbf{x}, p)}{\partial z} \left[2 \int_{-1}^{\mu} dy \, \frac{1 - y^{2}}{D_{\mu\mu}(y)} - \int_{-1}^{1} d\mu \, \frac{(1 - \mu)(1 - \mu^{2})}{D_{\mu\mu}(\mu)} \right],$$

$$g_{c}(\mathbf{x}, p, \mu) = -\frac{1}{2} \frac{\partial F(\mathbf{x}, p)}{\partial p} \left[2 \int_{-1}^{\mu} dy \, \frac{D_{\mu p}(y)}{D_{\mu\mu}(y)} - \int_{-1}^{1} d\mu \, \frac{(1 - \mu)D_{\mu p}(\mu)}{D_{\mu\mu}(\mu)} \right],$$
(7)

which is the sum of the so-called streaming (g_s) and interstellar Compton–Getting⁵ (g_c) anisotropies, determined by the gradients of the isotropic distribution function F(x, p) with respect to z and p, respectively.

In the same limit the isotropic distribution function F(x, p) obeys the general diffusion-convection transport equation

$$\frac{\partial}{\partial z} \kappa_{zz} \frac{\partial F}{\partial z} + \frac{1}{p^2} \frac{\partial}{\partial p} p^2 \kappa_{pp} \frac{\partial F}{\partial p} - \mathcal{R}F + S(\mathbf{x}, p)$$

$$= \frac{1}{4} \left[v \frac{\partial}{\partial z} H_0 \frac{\partial F}{\partial p} - \frac{1}{p^2} \frac{\partial}{\partial p} p^2 v H_0 \frac{\partial F}{\partial z} \right]$$

$$= \frac{1}{4} \left[v \frac{\partial H_0}{\partial z} \frac{\partial F}{\partial p} - \frac{1}{p^2} \frac{\partial}{\partial p} (p^2 v H_0) \frac{\partial F}{\partial z} \right] \tag{8}$$

with the diffusion coefficients

$$\kappa_{zz} = \frac{v^2 K_0}{8}, \quad \kappa_{pp} = \frac{1}{2} \int_{-1}^{1} d\mu \left[D_{pp}(\mu) - \frac{D_{\mu p}^2(\mu)}{D_{\mu \mu}(\mu)} \right], \quad (9)$$

and the anisotropy moments

$$K_0 = \int_{-1}^1 d\mu \, \frac{(1 - \mu^2)^2}{D_{\mu\mu}(\mu)}, \quad H_0 = \int_{-1}^1 d\mu \, \frac{(1 - \mu^2)D_{\mu\nu}(\mu)}{D_{\mu\mu}(\mu)}.$$
(10)

2.1. Maximum Relative Anisotropy

A quantity often used in comparison with observations is the maximum relative anisotropy

$$\delta(\mathbf{x}, p) = \frac{|f_0(\mathbf{x}, p, \mu = 1) - f_0(\mathbf{x}, p, \mu = -1)|}{f_0(\mathbf{x}, p, \mu = 1) + f_0(\mathbf{x}, p, \mu = -1)}$$

$$\simeq \frac{|g(\mathbf{x}, p, \mu = 1) - g(\mathbf{x}, p, \mu = -1)|}{2F(\mathbf{x}, p)},$$
(11)

where we use Equation (2) and $g \ll F$. According to Equation (7) this maximum relative anisotropy

$$\delta(\mathbf{x}, p) = \delta_s(\mathbf{x}, p) + \delta_c(\mathbf{x}, p) \tag{12}$$

is the sum of two parts: the streaming part

$$\delta_s(\mathbf{x}, p) = -\frac{v}{4} \frac{\partial \ln F(\mathbf{x}, p)}{\partial z} \int_{-1}^1 d\mu \, \frac{1 - \mu^2}{D_{\mu\mu}(\mu)} \tag{13}$$

and the interstellar Compton-Getting part

$$\delta_c(\mathbf{x}, p) = -\frac{1}{2} \frac{\partial \ln F(\mathbf{x}, p)}{\partial p} \int_{-1}^1 d\mu \, \frac{D_{\mu p}(\mu)}{D_{\mu \mu}(\mu)}. \tag{14}$$

3. Linearly Polarized Isospectral Slab Alfvenic Turbulence

There are four different slab Alvén waves: forward (f) and backward (b) propagating waves which each can be left-handed (LH) or right-handed (RH) circularly polarized, respectively. The cross and magnetic helicities

$$H_{c} = \frac{I_{f}(k_{\parallel}) - I_{b}(k_{\parallel})}{I_{f}(k_{\parallel}) + I_{b}(k_{\parallel})} \in [-1, 1],$$

$$\sigma_{f,b} = \frac{I_{f,b,\text{LH}}(k_{\parallel}) - I_{f,b,\text{RH}}(k_{\parallel})}{I_{f,b,\text{LH}}(k_{\parallel}) + I_{f,b,\text{RH}}(k_{\parallel})} \in [-1, 1]$$
(15)

indicate the relative fraction of forward and backward waves in the total intensity $I_{\text{total}}(k_{\parallel}) = I_f(k_{\parallel}) + I_b(k_{\parallel})$ and the relative fraction of LH and RH polarized waves, respectively.

⁵ The terminology "interstellar Compton–Getting anisotropy" used here in reference to the net weighted Alfvén wave speed is technically correct, but somewhat misleading as in the conventional context of cosmic ray transport the Compton–Getting anisotropy refers to the dipole anisotropy induced by the relative motion of the observer with respect to the interstellar medium.

For undamped slab Alfvén waves the Fokker–Planck coefficients are given by (Schlickeiser 2002, Ch. 13)

$$\begin{cases}
D_{\mu\mu}(\mu) \\
D_{\mu p}(\mu) \\
D_{pp}(\mu)
\end{cases} = \sum_{j=\pm 1} \begin{cases}
(1 - j\epsilon\mu)^2 \\
j\epsilon p(1 - j\epsilon\mu) \\
\epsilon^2 p^2
\end{cases} D(j), \tag{16}$$

where j = 1 refers to forward moving Alfvén waves and j = -1 refers to backward moving Alfvén waves, respectively. Moreover,

$$D(j) = \frac{\pi^2 v (1 - \mu^2)}{2R_L^2 B_0^2 |\mu - j\epsilon|} [(1 - \sigma_j(k_r^j))(1 + H_c(k_r^j))I_{\text{total}}(k_r^j) + (1 + \sigma_j(-k_r^j))(1 + H_c(-k_r^j))I_{\text{total}}(-k_r^j)]$$

$$(17)$$

and

$$k_r^j = \frac{1}{R_L(\mu - j\epsilon)} \tag{18}$$

denotes the resonant wavenumber.

Guided by interplanetary and interstellar turbulence measurements we adopt power-law type wave intensities

$$I_{\text{total}}(k_{\parallel}) = I_0 k_{\parallel}^{-s} \Theta(k_{\parallel} - k_{\text{min}}) \Theta(k_{\text{max}} - k_{\parallel}),$$

$$I_0 = \frac{(\delta B)^2}{4\pi} \frac{s - 1}{k_{\text{min}}^{1-s} - k_{\text{max}}^{1-s}} \simeq \frac{s - 1}{4\pi} (\delta B)^2 k_{\text{min}}^{s-1}$$
(19)

for positive $k_{\parallel} \geqslant k_{\min} > 0$ with $s \in [1, 2)$. The case s = 5/3 represents Kolgomorov-type turbulence; the case s = 1 is referred to as hard-sphere scattering. Moreover, we adopt isospectral turbulence, that the same spectral index s holds for the intensities of all four waves. In this case the cross and magnetic helicities are constants independent of wavenumber.

With both forward and backward moving waves present, the maximum resonant wavenumber (18) for cosmic ray hadrons with mass (A) and charge (Q_a) numbers and Lorentz factor γ occurs at about the inverse ion skin depth,

$$k_{r,\text{max}} = k_r^j(\mu = 0) = \frac{1}{R_L \epsilon} = \frac{\Omega_a}{V_A} = \frac{\omega_{p.i}}{c} \frac{Q_a}{A\gamma}.$$
 (20)

Consequently, the maximum resonant Alfvén wave frequency is given by

$$\omega_{R,\text{max}} = V_{A} k_{r,\text{max}} = \Omega_{a} = \Omega_{p,0} \frac{Q_{a}}{A \gamma}, \tag{21}$$

which for Lorentz factors and charge/mass ratios lies well within the Alfvenic range of turbulence $\omega_R \leqslant \Omega_{p,0}$.

We introduce the maximum cosmic ray momentum with $q_a = Q_a e$

$$p_m = \frac{|Q_a|eB_0}{k_{\min}c} = 1.5 \cdot 10^3 |Q_a|B_0(\mu G) \lambda_{10} \frac{\text{TeV}}{c}, \quad (22)$$

where $\lambda_{\text{max}} = 2\pi k_{\text{min}}^{-1} = 10\lambda_{10}$ pc denotes the maximum wavelength of the Alfvén waves in the interstellar medium.

We then obtain for momenta $p \leq p_m$

$$D(1) = (1 + H_c)D_0(p)(1 - \mu^2)$$

$$\times [(1 - \sigma_f)(\mu - \epsilon)^{s-1}\Theta(\mu - \epsilon)$$

$$+ (1 + \sigma_f)(\epsilon - \mu)^{s-1}\Theta(\epsilon - \mu)],$$

$$D(-1) = (1 - H_c)D_0(p)(1 - \mu^2)$$

$$\times [(1 - \sigma_b)(\mu + \epsilon)^{s-1}\Theta(\mu + \epsilon)$$

$$+ (1 + \sigma_b)(-(\mu + \epsilon))^{s-1}\Theta(-(\mu + \epsilon))]$$
 (23)

with

$$D_{0}(p \leq p_{m}, 1 < s < 2)$$

$$= \frac{\pi(s-1)vk_{\min}}{8} \frac{(\delta B)^{2}}{B_{0}^{2}} (R_{L}k_{\min})^{s-2}$$

$$= \frac{\pi(s-1)vk_{\min}}{8} \frac{(\delta B)^{2}}{B_{0}^{2}} \left(\frac{p}{p_{m}}\right)^{s-2}, \tag{24}$$

whereas for hard-sphere scattering

$$D_0(p \leqslant p_m, s = 1) = \frac{\pi v k_{\min}}{8 \ln(k_{\max}/k_{\min})} \frac{(\delta B)^2}{B_0^2} \left(\frac{p}{p_m}\right)^{-1}.$$
 (25)

For greater momenta $p > p_m$ the functions $D_0(p > p_m) = 0$. With Equations (23)–(25) we find for the Fokker–Planck coefficients (16)

$$\begin{cases}
D_{\mu\mu}(\mu) \\
D_{\mu p}(\mu) \\
D_{pp}(\mu)
\end{cases} = \begin{cases}
(1 - \epsilon \mu)^2 D(1) + (1 + \epsilon \mu)^2 D(-1) \\
\epsilon p \left[(1 - \epsilon \mu) D(1) - (1 + \epsilon \mu) D(-1) \right] \\
\epsilon^2 p^2 \left[D(1) + D(-1) \right]
\end{cases} (26)$$

3.1. Linearly Polarized Alfvén Waves

For linearly polarized Alfvén waves $\sigma_{f,b} = 0$ the Fokker–Planck coefficients (26) simplify to

$$D_{\mu\mu}(\mu) = D_{0}(p, s)(1 - \mu^{2})[(1 + H_{c})|\mu - \epsilon|^{s-1}(1 - \epsilon\mu)^{2} + (1 - H_{c})|\mu + \epsilon|^{s-1}(1 + \epsilon\mu)^{2}],$$

$$D_{\mu\rho}(\mu) = D_{0}(p, s)(1 - \mu^{2})\epsilon p[(1 + H_{c})|\mu - \epsilon|^{s-1}(1 - \epsilon\mu) - (1 - H_{c})|\mu + \epsilon|^{s-1}(1 + \epsilon\mu)].$$

$$D_{pp}(\mu) = D_{0}(p, s)(1 - \mu^{2})\epsilon^{2}p^{2}[(1 + H_{c})|\mu - \epsilon|^{s-1} + (1 - H_{c})|\mu + \epsilon|^{s-1}].$$
(27)

For energetic cosmic ray particles $\epsilon \ll 1$ and turbulence spectral indices s < 2 the general calculations of Dung & Schlickeiser (1990a, 1990b) demonstrate that the Fokker–Planck coefficients (27) are well approximated by

$$D_{\mu\mu}(\mu) \simeq 2D_0(1-\mu^2)|\mu|^{s-1}[1-2H_c\,\epsilon\mu+\epsilon^2\mu^2],$$

$$D_{\mu p}(\mu) \simeq 2D_0(1-\mu^2)\,\epsilon\,p|\mu|^{s-1}(H_c-\epsilon\mu),$$

$$D_{pp}(\mu) = 2D_0(1-\mu^2)\,\epsilon^2p^2\mu|^{s-1}.$$
(28)

3.2. Diffusion-convection Transport Equation

With the approximations (28) we obtain to lowest order in $\epsilon \ll 1$ for the moments (10)

$$K_{0} \simeq \frac{1}{2D_{0}} \int_{-1}^{1} d\mu \, \frac{(1-\mu^{2})|\mu|^{1-s}}{1-2H_{c}\epsilon\mu+\epsilon^{2}\mu^{2}}$$

$$\simeq \frac{1}{D_{0}} \int_{0}^{1} d\mu \, (1-\mu^{2})\mu^{1-s} = \frac{2}{D_{0}(2-s)(4-s)},$$

$$H_{0} \simeq \epsilon p \int_{-1}^{1} d\mu \, \frac{(1-\mu^{2})(H_{c}-\epsilon\mu)}{1-2H_{c}\epsilon\mu+\epsilon^{2}\mu^{2}}$$

$$\simeq \epsilon p H_{c} \int_{-1}^{1} d\mu \, (1-\mu^{2}) + \mathcal{O}(\epsilon^{3}) \simeq \frac{4}{3} \epsilon p H_{c}. \tag{29}$$

The spatial diffusion coefficient in Equation (9) then becomes

$$\kappa_{zz}(p, 1 < s < 2) = \frac{v\lambda_{zz}}{3} = \frac{v^2}{4(2 - s)(4 - s)D_0(p)}$$

$$= \frac{v\lambda_{\text{max}}}{\pi^2(s - 1)(2 - s)(4 - s)} \frac{B_0^2}{(\delta B)^2} \left(\frac{p}{p_m}\right)^{2 - s}$$

$$= 9.4 \cdot 10^{28} \frac{\lambda_{10}}{(s - 1)(2 - s)(4 - s)} \frac{B_0^2}{(\delta B)^2} \beta$$

$$\times \left(\frac{p}{p_m}\right)^{2 - s} \text{cm}^2 \text{s}^{-1}, \tag{30}$$

with $\beta = v/c$ for 1 < s < 2, whereas for hard-sphere scattering

$$\kappa_{zz}(p, s = 1) = \frac{v^2}{12D_0(p, s = 1))}$$

$$= \frac{4v\lambda_{\text{max}}}{3\pi^2 \ln(k_{\text{max}}/k_{\text{min}})} \frac{B_0^2}{(\delta B)^2} \left(\frac{p}{p_m}\right)$$

$$\simeq 4.6 \cdot 10^{27} \lambda_{10} \frac{B_0^2}{(\delta B)^2} \beta \left(\frac{p}{p_m}\right) \text{cm}^2 \text{s}^{-1}, \quad (31)$$

where we use $k_{\rm max}=\omega_{p,i}/c$ so that $k_{\rm max}/k_{\rm min}=\lambda_{\rm max}\,\omega_{p,i}/2\pi c=1.15\cdot 10^{11}\lambda_{\rm l0}/n_i^{1/2}$ and $\ln(k_{\rm max}/k_{\rm min})\simeq 28.4+\ln\lambda_{\rm l0}-0.5\ln n_i$, where n_i denotes the ionized gas density. For linearly polarized slab Alfvén waves both spatial diffusion coefficients (30)–(31) are independent from the cross-helicity.

Likewise, we obtain for the momentum diffusion coefficient in Equation (9)

$$\kappa_{pp}(p) \simeq 2D_{0}(p) \epsilon^{2} p^{2} \int_{-1}^{1} d\mu \, (1 - \mu^{2}) |\mu|^{s-1} \\
\left[1 - \frac{(H_{c} - \epsilon \mu)^{2}}{1 - 2H_{c} \epsilon \mu + \epsilon^{2} \mu^{2}} \right] \\
= 2D_{0}(p) \epsilon^{2} p^{2} (1 - H_{c}^{2}) \int_{-1}^{1} d\mu \, \frac{(1 - \mu^{2}) |\mu|^{s-1}}{1 - 2H_{c} \epsilon \mu + \epsilon^{2} \mu^{2}} \\
\simeq 4D_{0}(p) \epsilon^{2} p^{2} (1 - H_{c}^{2}) \int_{0}^{1} d\mu \, (1 - \mu^{2}) \mu^{s-1} \\
= \frac{8D_{0}(p) \epsilon^{2} p^{2} (1 - H_{c}^{2})}{s(s+2)} = \frac{2(1 - H_{c}^{2}) V_{A}^{2} p^{2}}{s(4 - s)(4 - s^{2}) \kappa_{zz}(p)}, \quad (32)$$

where we used Equation (30) to express $D_0(p)$ in terms of $\kappa_{zz}(p)$. H_0 from Equation (29) provides $\partial H_0/\partial z \propto d(\epsilon)/dz \propto dV_{\rm A}/dz = 0$ and

$$\frac{1}{4p^2}\frac{\partial}{\partial p}(p^2vH_0) \simeq \frac{H_c}{3p^2}\frac{\partial}{\partial p}(V_{\rm A}p^3) = H_cV_{\rm A}.$$
 (33)

The diffusion-convection transport Equation (8) then reads

$$\frac{\partial}{\partial z} \left[\kappa_{zz}(p) \frac{\partial F}{\partial z} + H_c V_A F \right]
+ \frac{1}{p^2} \frac{\partial}{\partial p} \left[\frac{2(1 - H_c^2) V_A^2 p^4}{s(4 - s)(4 - s^2) \kappa_{zz}(p)} \frac{\partial F}{\partial p} \right]
- \mathcal{R}F + S(\mathbf{x}, p) = 0.$$
(34)

The diffusion-convection transport Equation (34) indicates correctly that momentum diffusion of particles only occurs for cross-helicity values different from ± 1 . Both forward and backward moving waves have to be present⁶ in order to obtain a finite value of κ_{pp} .

Moreover, the diffusion-convection transport Equation (34) indicates a net cosmic ray convection speed H_cV_A although the interstellar medium has been assumed to be at rest. This is easy to understand: the cosmic ray particles do not directly interact with the interstellar gas. Instead they undergo resonant interactions with the Alfvén waves carried by the interstellar gas. The forward and backward moving Alfvén waves themselves propagate with speeds $+V_A$ and $-V_A$, respectively, through the interstellar medium. The net cosmic ray convection speed H_cV_A is the weighted net speed of the slab Alfvén waves.

3.3. Maximum Relative Anisotropy

Likewise, the approximations (28) yield to lowest order in $\epsilon \ll 1$ for the maximum relative streaming and interstellar Compton–Getting anisotropies (13)–(14)

$$\delta_{s}(\mathbf{x}, p) = -\frac{v}{4D_{0}(p)(2 - s)} \frac{\partial \ln F(\mathbf{x}, p)}{\partial z}$$
$$= -\frac{(4 - s)\kappa_{zz}(p)}{v} \frac{\partial \ln F(\mathbf{x}, p)}{\partial z}$$
(35)

and

$$\delta_c(\mathbf{x}, p) = -\epsilon H_c p \frac{\partial \ln F(\mathbf{x}, p)}{\partial p}.$$
 (36)

⁶ If only one type of wave was present (either forward or backward moving) we could make a Lorentz coordinate transformation into the rest frame of these waves, where the turbulent electric fields of these waves would vanish. Without electric fields, momentum, diffusion of particles is absent. Obviously, such a Lorentz transformation into a coordinate system, where all turbulent electric fields vanish, is not possible if both forward and backward moving waves are present.

3.4. Anisotropy

For the μ -dependent anisotropy we use the approximations (28) to calculate to lowest order in $\epsilon \ll 1$ the integrals

$$\int_{-1}^{\mu} dy \, \frac{1 - y^{2}}{D_{\mu\mu}(y)} \simeq \frac{1}{2D_{0}} \int_{-1}^{\mu} dy \, |y|^{1-s}$$

$$= \frac{1}{2(2 - s)D_{0}} \begin{cases} 1 - (-\mu)^{2-s} & \text{for } \mu \leq 0 \\ 1 + \mu^{2-s} & \text{for } \mu \geq 0 \end{cases} \end{cases},$$

$$\int_{-1}^{1} d\mu \, \frac{(1 - \mu)(1 - \mu^{2})}{D_{\mu\mu}(\mu)} \simeq \frac{1}{2D_{0}} \int_{-1}^{1} dy \, (1 - y)|y|^{1-s}$$

$$= \frac{1}{D_{0}(2 - s)}.$$

$$\int_{-1}^{\mu} dy \, \frac{D_{\mu\rho}(y)}{D_{\mu\mu}(y)} \simeq \epsilon \, p \left[H_{c}(\mu + 1) + \frac{(2H_{c} - 1)\epsilon}{2} (\mu^{2} - 1) \right],$$

$$\int_{-1}^{1} dy \, \frac{(1 - y)D_{\mu\rho}(y)}{D_{\mu\mu}(y)} \simeq 2\epsilon \, pH_{c}.$$
(37)

The streaming anisotropy in Equation (7) then becomes

$$g_{s}(\mathbf{x}, p, \mu) = -\frac{v}{4(2 - s)D_{0}(p)} \frac{\partial F(\mathbf{x}, p)}{\partial z}$$

$$\times \left\{ -(-\mu)^{2-s} \text{ for } \mu \leq 0 \right\}$$

$$= -\frac{(4 - s)\kappa_{zz}}{v} \frac{\partial F(\mathbf{x}, p)}{\partial z} |\mu|^{2-s} \operatorname{sgn}(\mu). \tag{38}$$

Likewise, the interstellar Compton–Getting anisotropy in Equation (7) reads

$$g_{c}(\mathbf{x}, p, \mu) = -\epsilon p \frac{\partial F(\mathbf{x}, p)}{\partial p} [H_{c}\mu + \frac{(2H_{c} - 1)\epsilon}{2} (\mu^{2} - 1)]$$

$$\simeq -\epsilon H_{c}\mu p \frac{\partial F(\mathbf{x}, p)}{\partial p},$$
(39)

where the last approximation holds for nonzero cross helicities. Most noteworthy are the different μ -dependences of the two anisotropies. The streaming anisotropy is proportional to $\propto |\mu|^{2-s} \operatorname{sgn}(\mu)$. For the Kolmogorov turbulence spectral index s=5/3 we obtain $g_s(\mu) \propto |\mu|^{1/3} \operatorname{sgn}(\mu)$. This is markedly different from the much weaker μ -dependence of the interstellar Compton–Getting anisotropy $g_c(\mu) \propto \mu$.

3.5. Local Interstellar Cosmic Ray Anisotropy

Cosmic rays at momenta much larger than about $10\,\mathrm{GeV}/c$ are not affected by the interplanetary solar wind magnetic turbulence, as the maximum solar wind turbulence wavelength is much smaller than the gyroradius of the relativistic galactic cosmic rays. Consequently, no solar modulation of galactic cosmic rays with momenta much larger than about $10\,\mathrm{GeV}/c$ is observed.

It has been demonstrated by Zhang et al. (2014) and Zhang & Pogorelov (2017) that the pristine galactic anisotropy of relativistic cosmic rays with TeV energies in the local interstellar medium can be derived from using Liouville's theorem to map the observed cosmic ray anisotropies at Earth back to the local interstellar medium. This requires the knowledge of the guide magnetic field configuration as

calculated from magnetohydrodynamic model heliospheres. This Liouville mapping technique is able to infer the μ -dependence of the pristine TeV cosmic ray anisotropy in the local interstellar medium (see Figure 1).

The observations shown in Figure 1 agree better with a linear dependence on μ . We therefore calculate in the following the local interstellar Compton–Getting and the streaming anisotropies of TeV cosmic rays.

4. Local Interstellar Compton-Getting Anisotropy

For the local interstellar Compton–Getting cosmic ray anisotropy we use the observed power-law momentum spectrum of galactic TeV cosmic rays $F_{\odot}(p) \propto p^{-\Gamma}$ with $\Gamma \simeq 4.7$. With Equation (39) we then obtain for the relative interstellar Compton–Getting anisotropy

$$\frac{g_{\odot,c}(p,\mu)}{F_{\odot}} = \Gamma \epsilon H_c \mu = \frac{V_{\rm A} \Gamma H_c \mu}{c \beta}.$$
 (40)

For relativistic cosmic ray momenta ($\beta \simeq 1$)

$$\frac{g_{\odot,c}(p,\mu)}{F_{\odot}(p)} = \frac{V_{\rm A}\Gamma}{c}H_c\mu = 1.6 \cdot 10^{-3}V_{\rm A}(10^7 \,\mathrm{cm \,s^{-1}})H_c\mu. \tag{41}$$

In Figure 2 we plot the local relative interstellar Compton–Getting anisotropy as a function of μ for different cross-helicity values.

We emphasize that the relative interstellar Compton–Getting anisotropy (1) of relativistic cosmic rays is independent of momentum as long as the local interstellar cosmic ray momentum spectrum is a straight power law. If the latter shows spectral curvature the relative interstellar Compton–Getting anisotropy directly reflects this spectral curvature because then

$$\frac{g_{\odot,c}(p,\mu)}{F_{\odot}(p)} = 3.3 \cdot 10^{-4} V_{\rm A} (10^7 \,\mathrm{cm s}^{-1}) \left[\frac{\partial \ln F_{\odot}(p)}{\partial \ln p} \right] H_c \mu. \tag{42}$$

This spectral curvature in Equation (42) can explain the observed momentum dependence of the local cosmic ray anisotropy shown in the bottom part of Figure 7 of Ahlers & Mertsch (2017).

We note that the local maximum relative interstellar Compton–Getting anisotropy (36) is given by

$$\delta_{\odot,c} = -\epsilon H_c p \frac{\partial \ln F(\mathbf{x}, p)}{\partial p} = \frac{|g_{\odot,c}(\mu = 1)|}{F_{\odot}(p)}$$
$$\simeq \Gamma |H_c| \frac{V_A}{c} = 1.6 \cdot 10^{-3} |H_c| V_A (10^7 \text{ cm s}^{-1}). \tag{43}$$

It is independent of momentum as long as the local interstellar cosmic ray momentum spectrum is a straight power law. Its constant value is in excellent agreement with the observations of $\delta_{\odot} = 10^{-3}$, shown in Figure 1 of Mertsch & Funk (2015). The observed anisotropy suggests values of

$$|H_c|V_{\Delta}(10^7 \text{ cm s}^{-1}) = 0.62.$$
 (44)

which are highly reasonable for values of $|H_c|$ close to unity. Realistic values are indeed extreme values of $H_c = -1$ (only backward moving waves present) and $H_c = 1$ (only forward

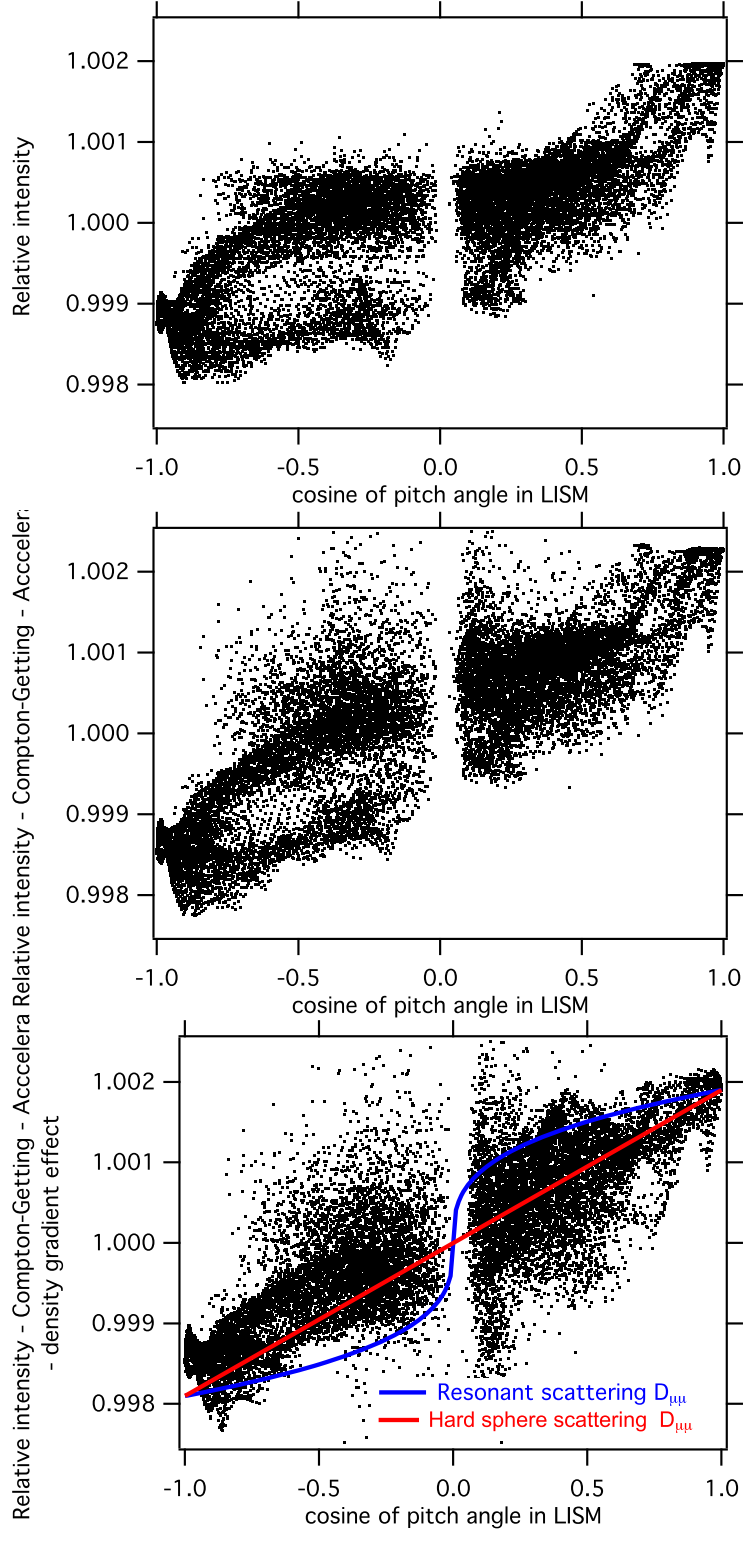


Figure 1. Distribution of the relative density $1 + (g(\mu)/F)$ of cosmic rays with energy of 4 TeV as a function of μ in the local interstellar medium. The top panel is the measured relative intensity from the Tibet airshower array (Amenomori et al. 2006) after backtracking the data into the interstellar medium. The middle panel results after correcting for the Compton–Getting or acceleration effect due to the regular solar system movement around the galactic center. There are no particles at $\mu=0$, because they never get into the heliosphere from the strict particle trajectory calculations. The bottom panel is obtained from the Liouville mapping technique, which uses a detailed model of the heliospheric electromagnetic fields, adopting also the direction and strength (3 μ G) of the ambient uniform local interstellar magnetic field. The bottom diagram indicates the true pristine cosmic ray pitch-angle anisotropy in the local interstellar medium. In the lowest diagram the blue line is the pitch-angle distribution $\propto |\mu|^{1/3} \operatorname{sgn}(\mu)$ expected from the streaming anisotropy with s=5/3 due to resonant wave-particle interactions. The red line is the fitted linear pitch-angle distribution $\propto \mu$, which agrees better with the observations. Such a linear dependence also results from the streaming anisotropy due to resonant wave-particle interactions under the hard-sphere scattering assumption (s=1).

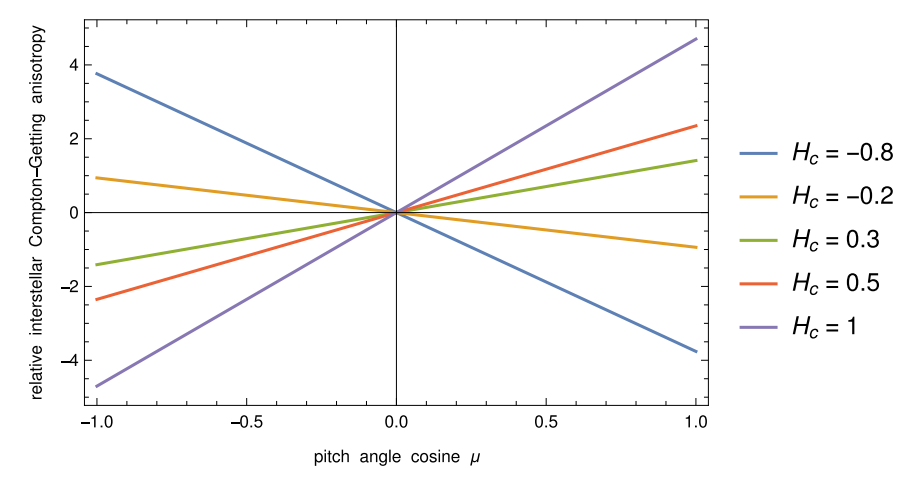


Figure 2. Interstellar relative Compton–Getting cosmic ray anisotropy $g_{\odot,c}(p,\mu)/F_{\odot}$ (in units of $\Gamma V_{\rm A}/c$ as a function of μ for different cross-helicity values $H_c=-0.8,\ -0.2,\ 0.3,\ 0.5,\ 1.$

moving waves present). In the interstellar medium we deal with self-generated Alfvén waves by anisotropic cosmic ray distribution functions (so-called cosmic ray self-confinement). Here it is relevant that the growth/damping rates of forward-and backward moving slab Alfvén waves by the cosmic ray streaming anisotropy are different (Bell 1978; Vainio & Schlickeiser 1998): independent of the polarization state forward moving waves have a positive growth rate, whereas backward moving waves have a positive damping rate. This difference drives physical systems quickly to a state in which only unidirectional waves remain (Ko 1992, Appendix of Schlickeiser & Shalchi 2008). This is demonstrated clearly, e.g., in Sections 6 and 7 of Schlickeiser et al. (2016).

5. Local Streaming Anisotropy

With $\eta = 2 - s$ the local relative streaming anisotropy can be calculated from Equation (38) as

$$\frac{g_{\odot,s}(p,\mu)}{F_{\odot}(p)} = \alpha_{\odot}(\eta)|\mu|^{\eta}\operatorname{sgn}(\mu) \tag{45}$$

with the dimensionless quantity

$$\alpha_{\odot}(\eta) = -\frac{(2+\eta)\kappa_{zz}(p)}{c\beta} \left[\frac{\partial \ln F(z,p)}{\partial z} \right]_{\odot}.$$
 (46)

Equations (30)–(31) provide for relativistic cosmic rays in terms of the dimensionless momentum $x = p/m_pc$ and the constant scattering mean free path L_0

$$\kappa_{zz}(x) = K_0(\eta) x^{\eta} = \frac{c}{3} L_0 x^{\eta}, \quad L_0(0 < \eta < 1)$$

$$= 9.4 \cdot 10^{18} \cdot (6.3 \cdot 10^{-7})^{\eta} \frac{\lambda_{10}^{1-\eta}}{B_0^{\eta} (\mu \text{G}) \eta (1 - \eta) (2 + \eta)}$$

$$\times \left(\frac{B_0}{\delta B}\right)^2 \text{ cm},$$

$$L_0(\eta = 1) = \frac{2.9 \cdot 10^{11}}{B_0(\mu \text{G})} \left(\frac{B_0}{\delta B}\right)^2 \text{ cm}.$$
(47)

Especially for Kolmogorov turbulence with s = 5/3, we obtain $\eta = 1/3$ and

$$L_0\left(\frac{1}{3}\right) = 1.5 \cdot 10^{17} \frac{\lambda_{10}^{2/3}}{B_0^{1/3}(\mu \text{G})} \left(\frac{B_0}{\delta B}\right)^2 \text{ cm.}$$
 (48)

For relativistic cosmic rays the quantity (46) then reads

$$\alpha_{\odot}(\eta) = -\frac{(2+\eta)L_0 x^{\eta}}{3} \left[\frac{\partial \ln F(z,p)}{\partial z} \right]_{\odot},\tag{49}$$

or

$$\alpha_{\odot}(0 < \eta < 1) = -3.1 \cdot 10^{18} \frac{\lambda_{10}}{(s - 1)(2 - s)}$$

$$\times \frac{B_0^2}{(\delta B)^2} \left(\frac{p}{p_m}\right)^{2 - s} \left[\frac{\partial \ln F(z, p)}{\partial z}\right]_{\odot}$$

$$= -3.1 \cdot 10^{18} \cdot (6.3 \cdot 10^{-7})^{\eta}$$

$$\times \frac{\lambda_{10}^{1 - \eta}}{\eta (1 - \eta) B_0^{\eta}} \frac{B_0^2}{(\delta B)^2} x^{\eta} \left[\frac{\partial \ln F(z, p)}{\partial z}\right]_{\odot}$$
(50)

and in the hard-sphere case

$$\alpha_{\odot}(\eta = 1) = -2.9 \cdot 10^{11} \frac{B_0^2}{(\delta B)^2} \frac{x}{B_0(\mu \text{G})} \left[\frac{\partial \ln F(z, p)}{\partial z} \right]_{\odot}.$$
(51)

Obviously the parameter (49) is determined by the local galactic spatial gradient $[\partial F(z,p)/\partial z]_{\odot}$ at the position of the solar system. Unfortunately, this galactic spatial gradient cannot be directly observed. However, we can calculate this spatial gradient from the analytical solution of the diffusion-convection transport Equation (34). As we will demonstrate below the inferred theoretical value of the local galactic spatial gradient $[\partial F(z,p)/\partial z]_{\odot}$ at the position of the solar system depends sensitively on the adopted spatial distribution function $S_1(z)$ of cosmic ray sources in the transport Equation (34). We illustrate this essential point below by using the solution of Schlickeiser et al. (2014—hereafter referred to as SWK):

(1) For symmetric spatial source distributions $S_1(-z) = S_1(z)$ we expect rather small values of α_{\odot} due to the galactic location

of the Earth and solar system close or near to the galactic plane at z=0. Because of the adopted source distribution symmetry, all solutions of the diffusion-momentum transport Equation (34) exhibit the property $[\partial F/\partial z]_{z=0}=0$, which then implies $\alpha_{\odot}=0$ so that the local streaming anisotropy vanishes.⁷

(2) Nonzero values of the local galactic spatial gradient $[\partial F(z,p)/\partial z]_{\odot}$ only occur for nonsymmetric spatial source distributions with respect to the galactic plane. We illustrate this effect below using the simplified SWK-model, but assuming that only one point source of sub-PeV cosmic rays located at $z_i \neq 0$ exists in the galaxy. This single point source case has been suggested before by, e.g., Erlykin & Wolfendale (1997). We then calculate the resulting local streaming isotropy.

We consider both cases in turn.

5.1. The SWK-model

SWK modeled the transport of local galactic cosmic ray protons by the spatially one-dimensional steady-state diffusion transport equation

$$\kappa_{zz}(p)\frac{\partial^2 F(z,p)}{\partial z^2} + \frac{1}{p^2}\frac{\partial}{\partial p}[\dot{p}F(z,p)] = -S_1(z)S_2(x). \quad (52)$$

In comparison to our transport Equation (34) SWK only investigated the competition of momentum dependent spatial diffusion, continuous momentum losses, and injection by sources, but they ignored particle convection, momentum diffusion and catastrophic losses as less important processes. With reasonable assumptions on the momentum dependence of the spatial diffusion coefficient $\kappa_{zz}(p)$ SWK successfully explained the differential intensity spectrum of the local galactic cosmic ray protons observed by *Voyager* 1, justifying this simplified modeling.

The spatial variable z in Equation (52) refers to the spatial coordinate along the guide magnetic field, As noted by Blies & Schlickeiser (2012) the dimensionality of the spatial cosmic ray transport depends on the structure and disorder of the partially turbulent galactic magnetic field. In general, one has to discriminate between spatial diffusion along (parallel diffusion) and across (perpendicular diffusion) the ordered guide magnetic field. Parallel diffusion results from rapid pitch-angle scattering of cosmic ray particles by the fluctuating magnetic field component, whereas perpendicular diffusion can be caused by a variety of effects including gradient and curvature drifts in nonuniform guide magnetic fields combined with rapid pitch-angle scattering and by magnetic field line random walk. If perpendicular diffusion is negligibly small, the onedimensional spatial transport is appropriate, implying that the cosmic ray sources and the solar system are well connected on the same magnetic flux tube. If the local ordered magnetic field is inclined with the constant nonzero angle ψ with respect to the galactic plane one finds that $z = z_g \sin \psi$, where z_g is the galactic height. For ease of exposition we adopt this onedimensional spatial transport model here as in SWK. Because of the highly flattened disk shape of the Galaxy, the radial spatial gradients are much smaller than the perpendicular gradient with respect to the galactic height z_g (note that these gradients enter the diffusion transport equation). This also justifies the one-dimensional spatial transport model. In the following we refer to z simply as galactic distance from the plane, with the understanding that strictly $z=z_g\sin\psi$.

In terms of the normalized momentum $x = p/(Am_pc)$ the transport Equation (52) for relativistic cosmic ray protons reads

$$K_0 x^{\eta} \frac{\partial^2 F(z, x)}{\partial z^2} + \frac{1}{x^2} \frac{\partial}{\partial x} [B(x) x^2 F(z, x)] = -S_1(z) S_2(x),$$
(53)

where

$$B(x) = \frac{x}{\tau_0}$$
, $\tau_0 = 5.4 \cdot 10^7 n^{-1} \text{ yr} = 1.7 \cdot 10^{15} n^{-1} \text{ s}$ (54)

denotes the relevant momentum loss rate due to pion production losses in inelastic hadron-hadron collisions in the interstellar medium of number density n. According to SWK the general solution of the transport Equation (53) for the spatial boundary conditions $F(z=\pm\infty,x)=0$ and the momentum boundary condition $F(z,x=\infty)=0$ then is given by

$$F(z, x) = \frac{1}{2\pi^{1/2}B(x)} \int_{-\infty}^{\infty} dz_0 \, S_1(z_0)$$

$$\times \int_{x}^{\infty} dx_0 \, \frac{S_2(x_0)e^{-\frac{(z-z_0)^2}{4W_d^2(x,x_0)}}}{W_d(x, x_0)}, \tag{55}$$

in terms of the effective diffusion function length⁸

$$W_d(x, x_0) = \left[K_0 \int_x^{x_0} dt \, \frac{\kappa(t)}{B(t)} \right]^{1/2} = \left[\frac{K_0 \tau_0}{\eta} (x_0^{\eta} - x^{\eta}) \right]^{1/2}$$
$$= L_d(\eta) x^{\frac{\eta}{2}} \sqrt{\left(\frac{x_0}{x}\right)^{\eta} - 1}$$
(56)

with

$$L_d(\eta) = \sqrt{\frac{K_0 \tau_0}{\eta}} = \frac{4.1}{\eta} \sqrt{\frac{(6.3 \cdot 10^{-7})^{\eta} \lambda_{10}^{1-\eta} B_0^{2-\eta}}{(1-\eta)(2+\eta)n(\delta B)^2}} \text{ kpc.} \quad (57)$$

For the Kolmogorov value we obtain

$$L_d\left(\frac{1}{3}\right) = 910\sqrt{\frac{\lambda_{10}^{2/3}}{nB_0^{1/3}(\mu G)}\frac{B_0^2}{(\delta B)^2}} \text{ pc},$$
 (58)

while in the hard-sphere scattering case

$$L_d(1) = 0.72 \sqrt{\frac{B_0^2}{n(\delta B)^2 B_0(\mu G)}} \text{ pc.}$$
 (59)

5.2. Symmetric Spatial Source Distribution

As SWK we adopt as injection conditions a spatially homogeneous layer of cosmic ray sources within the maximum distance $z_u \simeq 200$ pc (solar system inside of the source

⁷ In fact $[\partial F/\partial z]_{z=0} = 0$ is often used as one spatial boundary condition when solving the transport Equation (34) for symmetric spatial source distributions.

Our notation is slightly different from SWK: our W_d equals $\sqrt{W_d$ SWK.

distribution), injecting the same momentum power law, i.e.,

$$S_1(z) = \Theta[z_u - |z|], \quad S_2(x) = S_0 x^{-\Gamma_0}$$
 (60)

with the step function Θ and spectral index value $\Gamma_0 > 3$. The solution (55) then reads

$$F(z, x) = \frac{S_0 \tau_0}{2\pi^{1/2} x} \int_x^{\infty} dx_0 \, \frac{x_0^{-\Gamma_0}}{W_d(x, x_0)} \int_{-(z_u + z)}^{z_u - z} dZ \, e^{-\frac{Z^2}{4W_d^2(x, x_0)}}$$

$$= \frac{S_0 \tau_0}{2x} \int_x^{\infty} dx_0 \, x_0^{-\Gamma_0}$$

$$\times \left[\text{erf} \left(\frac{z_u - z}{2W_d(x, x_0)} \right) + \text{erf} \left(\frac{z_u - z}{2W_d(x, x_0)} \right) \right]. \tag{61}$$

From Equation (61) we readily find the spatial gradient

$$\frac{\partial F(z,x)}{\partial z} = \frac{-S_0}{2\pi^{1/2}x} \int_x^\infty dx_0 \, \frac{x_0^{-\Gamma_0}}{W_d(x,x_0)} \\
\times \left[e^{-\left(\frac{z_u-z}{2W_d(x,x_0)}\right)^2 - e^{-\left(\frac{z_u+z}{2W_d(x,x_0)}\right)^2} \right] \\
= -\frac{S_0}{\pi^{1/2}x} \int_x^\infty dx_0 \, \frac{x_0^{-\Gamma_0}}{W_d(x,x_0)} e^{-\frac{z_u^2+z^2}{4W_d^2(x,x_0)}} \sinh\left(\frac{zz_u}{4W_d^2(x,x_0)}\right). \tag{62}$$

The solar system is located in the galactic disk near z = 0, so that the local galactic spatial gradient (62) vanishes. Consequently, also the parameter (49) vanishes and the local streaming anisotropy (45) becomes zero. In this case the local cosmic ray anisotropy is solely determined by the interstellar Compton–Getting anisotropy (41) and (42).

Moreover, as the local streaming anisotropy vanishes, no galactic cosmic ray anisotropy problem, as described by Mertsch & Funk (2015), exists, and there is no reason to discard quasilinear cosmic ray transport theories.

5.3. Single Point Source

Here we adopt as injection conditions a single cosmic ray source at position z_i , injecting a momentum power law, i.e.,

$$S_1(z) = \delta(z - z_i), \quad S_2(x) = S_n x^{-q}$$
 (63)

with spectral index value q > 3. The solution (55) then reads

$$F(z,x) = \frac{S_p \tau_0}{2\pi^{1/2} x} \int_x^{\infty} dx_0 \, \frac{x_0^{-q}}{W_d(x,x_0)} e^{-\frac{(z-z_i)^2}{4W_d^2(x,x_0)}},\tag{64}$$

yielding readily

$$\frac{\partial F(z,x)}{\partial z} = -\frac{S_p \tau_0(z-z_i)}{4\pi^{1/2} x} \int_x^\infty dx_0 \, \frac{x_0^{-\Gamma_0}}{W_d^3(x,x_0)} e^{-\frac{(z-z_i)^2}{4W_d^2(x,x_0)}}.$$
(65)

Consequently,

$$\frac{\partial \ln F(z,x)}{\partial z} = -\frac{z - z_i}{2} \frac{\int_x^\infty dx_0 \, \frac{x_0^{-q}}{W_d^3(x,x_0)} e^{-\frac{(z-z_i)^2}{4W_d^2(x,x_0)}}}{\int_x^\infty dx_0 \, \frac{x_0^{-q}}{W_d(x,x_0)} e^{-\frac{(z-z_i)^2}{4W_d^2(x,x_0)}}}.$$
 (66)

Then at the position $z_{\odot} = 0$ of the solar system

$$\left[\frac{\partial \ln F(z,x)}{\partial z}\right]_{\odot} = \frac{z_i}{2} \frac{\int_x^{\infty} dx_0 \, \frac{x_0^{-q}}{W_d^3(x,x_0)} e^{-\frac{z_i^2}{4W_d^2(x,x_0)}}}{\int_x^{\infty} dx_0 \, \frac{x_0^{-q}}{W_d(x,x_0)} e^{-\frac{z_i^2}{4W_d^2(x,x_0)}}}.$$
 (67)

With the effective diffusion length (56) inserted we obtain for Equation (67)

$$\left[\frac{\partial \ln F(z,x)}{\partial z}\right]_{\odot} = \frac{z_{i}}{2L_{d}^{2}x^{\eta}} \frac{\int_{x}^{\infty} dx_{0} \frac{x_{0}^{-q}}{\left[\frac{x_{0}}{x}^{\eta}-1\right]^{3/2}} e^{-\frac{z_{i}^{2}}{4L_{d}^{2}x^{\eta}}\left[\frac{x_{0}}{x}^{\eta}-1\right]}}{\int_{x}^{\infty} dx_{0} \frac{x_{0}^{-q}}{\left[\frac{x_{0}}{x}^{\eta}-1\right]^{1/2}} e^{-\frac{z_{i}^{2}}{4L_{d}^{2}x^{\eta}}\left[\frac{x_{0}}{x}^{\eta}-1\right]}}$$

$$= \frac{z_{i}}{2L_{d}^{2}x^{\eta}} \frac{\int_{0}^{\infty} du \ u^{-\frac{1}{2}}\left(1+\frac{1}{u}\right)\frac{1-q}{\eta}-1e^{-\frac{z_{i}^{2}}{4L_{d}^{2}x^{\eta}}u}}{\int_{0}^{\infty} du \ u^{-\frac{3}{2}}\left(1+\frac{1}{u}\right)\frac{1-q}{\eta}-1e^{-\frac{\eta c_{i}^{2}}{4L_{d}^{2}x^{\eta}}u}}$$

$$= \frac{z_{i}}{2L_{d}^{2}x^{\eta}} \frac{\int_{0}^{\infty} du \ (1+u)^{\frac{1-q}{\eta}-1}u^{\frac{q-1}{\eta}-\frac{1}{2}}e^{-\frac{z_{i}^{2}}{4L_{d}^{2}x^{\eta}}u}},$$

$$\int_{0}^{\infty} du \ (1+u)^{\frac{1-q}{\eta}-1}u^{\frac{q-1}{\eta}-\frac{1}{2}}e^{-\frac{\eta c_{i}^{2}}{4L_{d}^{2}x^{\eta}}u},$$
(68)

where we substituted $u = [(x_0/x)^{\eta} - 1]^{-1}$. The two remaining integrals can be expressed in terms of confluent hypergeometric functions (Abramowitz & Stegun 1972), so that

$$\left[\frac{\partial \ln F(z,x)}{\partial z}\right]_{\odot} = \left[\frac{q-1}{\eta} + \frac{1}{2}\right] \frac{z_{i}}{2L_{d}^{2}x^{\eta}} \frac{U\left(\frac{q-1}{\eta} + \frac{3}{2}, \frac{3}{2}, \frac{z_{i}^{2}}{4L_{d}^{2}x^{\eta}}\right)}{U\left(\frac{q-1}{\eta} + \frac{1}{2}, \frac{1}{2}, \frac{z_{i}^{2}}{4L_{d}^{2}x^{\eta}}\right)}. \tag{69}$$

Then for single point source injection the dimensionless quantity (49) becomes

$$\alpha_{\odot}(\eta) = -\frac{(2+\eta)L_{0}z_{i}}{6L_{d}^{2}} \left[\frac{q-1}{\eta} + \frac{1}{2} \right] \frac{U\left(\frac{q-1}{\eta} + \frac{3}{2}, \frac{3}{2}, \frac{z_{i}^{2}}{4L_{d}^{2}x^{\eta}}\right)}{U\left(\frac{q-1}{\eta} + \frac{1}{2}, \frac{1}{2}, \frac{z_{i}^{2}}{4L_{d}^{2}x^{\eta}}\right)}$$

$$= -\frac{\left[q-1 + \frac{\eta}{2}\right](2+\eta)}{2} \frac{z_{i}}{c\tau_{0}} \frac{U\left(\frac{q-1}{\eta} + \frac{3}{2}, \frac{3}{2}, \frac{z_{i}^{2}}{4L_{d}^{2}x^{\eta}}\right)}{U\left(\frac{q-1}{\eta} + \frac{1}{2}, \frac{1}{2}, \frac{z_{i}^{2}}{4L_{d}^{2}x^{\eta}}\right)},$$
(70)

where we inserted L_d from Equation (57).

Using the Kummer transformation formula (13.1.29) in Abramowitz & Stegun (1972) Equation (70) can also be written as

$$\alpha_{\odot}(\eta) = -(2 + \eta) \left[\frac{q - 1}{\eta} + \frac{1}{2} \right] \frac{L_0 \operatorname{sgn}(z_i) x^{\frac{\eta}{2}}}{3L_d} \times \frac{U\left(\frac{q - 1}{\eta} + 1, \frac{1}{2}, \left(\frac{z_i}{z_c(\eta, x)}\right)^2\right)}{U\left(\frac{q - 1}{\eta} + \frac{1}{2}, \frac{1}{2}, \left(\frac{z_i}{z_c(\eta, x)}\right)^2\right)}$$
(71)

with the momentum dependent characteristic diffusion length

$$z_c(\eta, x) = 2L_d(\eta)x^{\frac{\eta}{2}}. (72)$$

We introduce the timescale

$$\tau_d(x) = \frac{\eta z_i^2}{4\kappa(x)} = \frac{\eta z_i^2}{4K_0(\eta)x^{\eta}},\tag{73}$$

which is the typical timescale for cosmic ray particles to spatially diffuse from the point source at z_i to the solar system at z = 0. In terms of the pion loss timescale (54) we note that the argument of the confluent hypergeometric functions in Equation (71) equals the ratio

$$\left(\frac{z_i}{z_c(x)}\right)^2 = \frac{\tau(x)}{\tau_0} = \left(\frac{x_c}{x}\right)^{\eta} \tag{74}$$

with the characteristic dimensionless momentum

$$x_c(\eta) = \left(\frac{z_i^2}{4L_d^2}\right)^{\frac{1}{\eta}}.$$
 (75)

For Kolmogorov turbulence

$$x_c \left(\frac{1}{3}\right) = 0.03 \left[\frac{n z_i^2 (\text{kpc}) B_0^{2/3} (\mu \text{G})}{\lambda_{10}^{2/3}} \left(\frac{\delta B}{B_0} \right)^2 \right]^3, \tag{76}$$

whereas for hard-sphere scattering

$$x_c(1) = 6.9 \cdot 10^5 n z_i^2 (\text{kpc}) n B_0(\mu \text{G}) \left(\frac{\delta B}{B_0}\right)^2.$$
 (77)

Hence, for point source distances smaller than $z_c(x)$, which is equivalent to momenta x greater than x_c , the diffusion time of cosmic ray particles is shorter than the pion loss time. Alternatively, for point source distances greater than $z_c(x)$, which is equivalent to momenta x smaller than x_c , the cosmic rays diffuse longer than the pion loss time.

We use the asymptotic expansions of the confluent hypergeometric functions for small and large arguments to derive

$$\left[\frac{q-1}{\eta} + \frac{1}{2}\right] \frac{U\left(\frac{q-1}{\eta} + 1, \frac{1}{2}, \left(\frac{z_{i}}{z_{c}(\eta, x)}\right)^{2}\right)}{U\left(\frac{q-1}{\eta} + \frac{1}{2}, \frac{1}{2}, \left(\frac{z_{i}}{z_{c}(\eta, x)}\right)^{2}\right)}$$

$$\simeq \left\{\frac{\Gamma\left(\frac{q-1}{\eta} + 1\right)}{\Gamma\left(\frac{q-1}{\eta} + \frac{1}{2}\right)} \text{ for } |z_{i}| \ll z_{c}(x) \text{ equivalent to } x \gg x_{c}$$

$$\left[\frac{q-1}{\eta} + \frac{1}{2}\right] \frac{z_{c}(x)}{|z_{i}|}; \text{ for } |z_{i}| \gg z_{c}(x) \text{ equivalent to } x \ll x_{c}\right\}.$$
(78)

Apart from factors of order unity, Equation (78) is well approximated by

$$\left[\frac{q-1}{\eta} + \frac{1}{2}\right] \frac{U\left(\frac{q-1}{\eta} + 1, \frac{1}{2}, \left(\frac{z_{i}}{z_{c}(\eta, x)}\right)^{2}\right)}{U\left(\frac{q-1}{\eta} + \frac{1}{2}, \frac{1}{2}, \left(\frac{z_{i}}{z_{c}(\eta, x)}\right)^{2}\right)}$$

$$\simeq \frac{z_{c}(x)}{z_{c}(x) + |z_{i}|} = \frac{2L_{d}x^{\frac{\eta}{2}}}{|z_{i}| + 2L_{d}x^{\frac{\eta}{2}}}.$$
(79)

With this approximation the quantity (71) varies as

$$\alpha_{\odot}(\eta) \simeq -\frac{2}{3}(2+\eta)L_{0}\operatorname{sgn}(z_{i})\frac{x^{\eta}}{z_{c}(x)+|z_{i}|} = -\frac{2}{3}(2+\eta)L_{0}\operatorname{sgn}(z_{i})\frac{x^{\eta}}{|z_{i}|+2L_{d}x^{\frac{\eta}{2}}}.$$
 (80)

Most noteworthy: for close source distances $|z_i| \ll z_c(x)$, or large momenta $x \gg x_c$, the quantity (80), apart from $\operatorname{sgn}(z_i)$, is independent of the actual value of $|z_i|$, and given by the ratio of the constant mean free path (47) and the effective diffusion length (57) as

$$\alpha_{\odot}(\eta, |z_i| \ll z_c(x)) \simeq \alpha_0 = -\frac{2+\eta}{3} \frac{L_0}{L_d} \operatorname{sgn}(z_i) x^{\frac{\eta}{2}}.$$
 (81)

Alternatively, for far source distances $|z_i| \gg z_c(x)$, or small momenta $x \ll x_c$, the quantity (80) decreases as

$$\alpha_{\odot}(\eta, |z| \ll z_c(x)) \simeq \frac{\alpha_0}{|z_i|},$$
 (82)

and therefore is always smaller than α_0 .

Numerically, we obtain for general values of nonzero η

$$\alpha_{\odot}(0 < \eta < 1) \simeq -\operatorname{sgn}(z_{i})(6.3 \cdot 10^{-7})^{\eta} \frac{\lambda_{10}^{1-\eta}}{\eta(1-\eta)B_{0}^{\eta}} \frac{B_{0}^{2}}{(\delta B)^{2}} \times \begin{cases} \frac{x_{2}^{\eta}}{L_{d}(\operatorname{pc})} & \text{for } |z_{i}| \ll z_{c}(x) \\ \frac{2x^{\eta}}{|z_{i}(\operatorname{pc})|}; & \text{for } |z_{i}| \gg z_{c}(x) \end{cases}$$
(83)

and in the hard-sphere case

$$\alpha_{\odot}(\eta = 1) = -\operatorname{sgn}(z_{i})9.4 \cdot 10^{-8} \frac{B_{0}^{2}}{(\delta B)^{2}} \frac{1}{B_{0}(\mu G)}$$

$$\begin{cases} \frac{x_{0}^{\frac{1}{2}}}{L_{d}(\operatorname{pc})} & \text{for } |z_{i}| \ll z_{c}(x) \\ \frac{2x}{|z_{i}(\operatorname{pc})|}; & \text{for } |z_{i}| \gg z_{c}(x) \end{cases}. \tag{84}$$

For the Kolmogorov case

$$\alpha_{\odot}\left(\frac{1}{3}\right) = -\operatorname{sgn}(z_{i})3.9 \cdot 10^{-2} \frac{\lambda_{10}^{2/3}}{B_{0}^{1/3}(\mu G)} \frac{B_{0}^{2}}{(\delta B)^{2}} \times \left\{ \frac{\frac{1}{z_{i}}}{L_{d}(\operatorname{pc})} \text{ for } |z_{i}| \ll z_{c}(x) \\ \frac{2x_{0}^{\frac{1}{3}}}{|z_{i}(\operatorname{pc})|}; \text{ for } |z_{i}| \gg z_{c}(x) \right\}.$$
(85)

We recall that the value of L_d depends on η , see Equations (57)–(59).

According to Equations (81)–(82) the maximum possible value of the parameter $\alpha_{\mathbb{Q}} \leq \alpha_{0}$ in the point source model are

$$\alpha_0(0 < \eta < 1) = -2.5 \cdot 10^{-4} \operatorname{sgn}(z_i) x^{\frac{\eta}{2}} \times \sqrt{\frac{n(2+\eta)}{1-\eta}} (6.3 \cdot 10^{-7})^{\eta/2} \frac{\lambda_{10}^{1-\eta}}{B_0^{\eta/2} (\mu \text{G})} \frac{B_0}{(\delta B)}$$
(86)

and

$$\alpha_0(\eta = 1) = -1.3 \cdot 10^{-7} \operatorname{sgn}(z_i) x^{\frac{1}{2}} \frac{B_0}{\delta B} \sqrt{\frac{n}{B_0(\mu G)}}.$$
 (87)

For the Kolmogorov case

$$\alpha_0 \left(\frac{1}{3}\right) = -4.3 \cdot 10^{-5} \operatorname{sgn}(z_i) x_0^{\frac{1}{6}} \frac{B_0}{\delta B} \sqrt{n} \frac{\lambda_{10}^{1/3}}{B_0^{1/6} (\mu G)}.$$
 (88)

Then, according to Equation (45), the maximum local relative streaming anisotropy for the single point source model is given by

$$\frac{g_{\odot,s,\max}(p,\mu)}{F_{\odot}(p)} = \alpha_0(\eta) |\mu|^{\eta} \operatorname{sgn}(\mu). \tag{89}$$

6. Summary and Conclusions

Starting from the Fokker–Planck description of cosmic ray transport we have derived the anisotropy of galactic cosmic rays in the interstellar medium at rest employing the diffusion approximation, which holds in astrophysical systems with the electromagnetic field ordering $B_0 \gg \delta B \gg \delta E$. This ordering is valid in the interstellar medium containing low-frequency magnetohydrodynamic linearly polarized slab Alfvén waves. We demonstrated that the anisotropy consists of two parts: the streaming anisotropy $g_s(z, p, \mu)$, caused by the spatial gradient of the isotropic part of the cosmic ray distribution function, and the interstellar Compton–Getting anisotropy $g_c(z, p, \mu)$, caused by the momentum gradient of the isotropic part of the cosmic ray distribution function.

For the case of linearly polarized Alfvén waves we calculate the dependencies of both anisotropies on the cosmic ray momentum p, cosmic ray pitch-angle cosine μ , and on the cross-helicity state H_c of the Alfvenic turbulence, characterizing the relative fraction of Alfvén waves moving parallel or antiparallel to the ordered magnetic guide field. First, the interstellar Compton-Getting anisotropy $g_c(z, p, \mu) \propto H_c \mu$ is independent of momentum and linearly proportional to $H_c\mu$. Second, the streaming anisotropy is independent from H_c and varies as $g_s(z, p, \mu) \propto (p|\mu|)^{\eta} \operatorname{sgn}(\mu)$ with $\eta = 2 - s$, where s denotes the power-law spectral index of interstellar turbulence. For Kolmogorov turbulence with s = 5/3we obtain $\eta = 1/3$ and $g_s(z, p, \mu) \propto (p|\mu|)^{1/3} \operatorname{sgn}(\mu)$. In the hard-sphere scattering case with s=1 one finds $g_s(z, p, \mu) \propto$ $p|\mu| \operatorname{sgn}(\mu)$. However, this increasing momentum dependence $\propto p$ is clearly ruled out by the observed momentum dependence (see Figure 7 of Ahlers & Mertsch 2017 of the local cosmic ray anisotropy at relativistic particle momenta.

These different pitch-angle dependencies can be tested by the Liouville mapping technique to infer the pristine interstellar cosmic ray anisotropy from measurements inside the solar system. For cosmic rays with energy of 4 TeV the derived pristine interstellar cosmic ray anisotropy shown in Figure 1 suggests the linear $(g \propto |\mu| \operatorname{sgn}(\mu))$ pitch-angle dependence. This is well explained by the interstellar Compton–Getting anisotropy, provided the Alfvén speed in the local interstellar

medium is about $62~\rm km~s^{-1}$. The implied near independence from the particle momentum also agrees favorably with the observed momentum dependence of the local cosmic ray anisotropy at relativistic particle momenta. The required local Alfvén speed of $62~\rm km~s^{-1}$ is about a factor of 2 higher than the Alfvén speed calculated with the observed electron density and magnetic field strength outside the solar system. However, the relativistic TeV cosmic rays arriving at Earth are about 10^6 years old, and have transversed a much larger volume in the galaxy. So what is of interest is the average Alfvén speed in that cosmic ray volume, which can be higher than $30~\rm km~s^{-1}$. For example, in the coronal phase of the ISM, occupying 90% of the volume, the electron density is as low as $10^{-3}~\rm cm^{-3}$, so that with a magnetic field strength of $1~\mu\rm G$, the Alfvén speed is $69~\rm km~s^{-1}$.

The linear pitch-angle dependence of the local interstellar anisotropy of 4 TeV cosmic rays can be explained by the streaming anisotropy only for the hard-sphere scattering case s = 1. However, this value of s = 1 implies an increasing momentum dependence $\propto p$, which is clearly ruled out by the observed momentum dependence of the local cosmic ray anisotropy at relativistic particle momenta.

Moreover, the streaming anisotropy $(\propto \partial F/\partial z)$ is proportional to the spatial gradient of the isotropic part of the cosmic ray distribution function. Due to the particular location of the solar system in the galactic plane (z = 0) the spatial gradient $(\partial F/\partial z)_0$ and therefore the local streaming anisotropy vanish for symmetric spatial source distribution with respect to galactic height z. Therefore, the galactic cosmic ray anisotropy problem as described by Mertsch & Funk (2015) does not exist. Finite values of the local streaming anisotropy only exist for nonsymmetric spatial source distributions with respect to the galactic plane. We illustrate this result adopting a single steady point source of sub-PeV cosmic rays. In the hard-sphere scattering case the single point source model also predicts an increasing momentum dependence (stronger than $\propto x^{1/2}$) of the local streaming anisotropy, which is ruled out by the observed momentum dependence of the local cosmic ray anisotropy at relativistic particle momenta.

This work relies on the quasilinear diffusion of cosmic rays caused by the resonant interactions with slab Alfvén waves. In future theoretical studies the implications of alternative transport theories on the cosmic ray anisotropy should be investigated, including nonresonant scattering and other types of nonslab turbulence. Moreover, the point source of sub-PeV cosmic rays can also be time-dependent. These topics will be left for future studies.

In conclusion, within the theoretical modeling presented in this work the local interstellar relative cosmic ray anisotropy is currently best explained by the interstellar Compton–Getting anisotropy. It is constant at relativistic particle momenta in excellent agreement with the observations at TeV energies, and it requires an Alfvén speed of about 62 km s⁻¹ in the local interstellar medium.

R.S. and J.O. acknowledge partial support by the Deutsche Forschungsgemeinschaft through grant Schl 201/34-1.

Appendix Anisotropy and Diffusion Approximation

For ease of exposition here we only consider isotropic source terms and isotropic momentum losses. With Equation (2) the Fokker–Planck Equation (3) becomes

$$v\mu \frac{\partial F}{\partial z} + v\mu \frac{\partial g}{\partial z} + \mathcal{R}F + \mathcal{R}g - S(\mathbf{x}, p, t)$$

$$= \frac{\partial}{\partial \mu} \left[D_{\mu\mu} \frac{\partial g}{\partial \mu} + D_{\mu\rho} \frac{\partial F}{\partial p} + D_{\mu\rho} \frac{\partial g}{\partial p} \right]$$

$$+ p^{-2} \frac{\partial}{\partial p} p^{2} \left[D_{\mu\rho} \frac{\partial g}{\partial \mu} + D_{p\rho} \frac{\partial F}{\partial p} + D_{p\rho} \frac{\partial g}{\partial p} \right]. \tag{90}$$

Averaging this equation over μ using Equation (6) yields

$$\frac{v}{2} \frac{\partial}{\partial z} \int_{-1}^{1} d\mu \mu g + \mathcal{R}F - S(\mathbf{x}, p, t)$$

$$= \frac{1}{2p^{2}} \frac{\partial}{\partial p} p^{2} \int_{-1}^{1} d\mu \left[D_{\mu p} \frac{\partial g}{\partial \mu} + D_{pp} \frac{\partial F}{\partial p} + D_{pp} \frac{\partial g}{\partial p} \right] \quad (91)$$

involving different moments of the anisotropy. In the derivation of Equation (91) we have used

$$D_{\mu\mu}(\mu = \pm 1) = D_{\mu\rho}(\mu = \pm 1) = 0.$$
 (92)

Subtracting Equation (91) from the full Fokker–Planck Equation (90) provides

$$v\mu \frac{\partial F}{\partial z} + v\mu \frac{\partial g}{\partial z} - \frac{v}{2} \frac{\partial}{\partial z} \int_{-1}^{1} d\mu \mu g + \mathcal{R}F$$

$$= \frac{\partial}{\partial \mu} \left[D_{\mu\mu} \frac{\partial g}{\partial \mu} + D_{\mu\rho} \frac{\partial F}{\partial p} + D_{\mu\rho} \frac{\partial g}{\partial p} \right]$$

$$+ p^{-2} \frac{\partial}{\partial p} p^{2} \left[D_{\mu\rho} \frac{\partial g}{\partial \mu} + D_{p\rho} \frac{\partial F}{\partial p} + D_{p\rho} \frac{\partial g}{\partial p} \right]$$

$$- \frac{1}{2p^{2}} \frac{\partial}{\partial p} p^{2} \int_{-1}^{1} d\mu \left[D_{\mu\rho} \frac{\partial g}{\partial \mu} + D_{p\rho} \frac{\partial F}{\partial p} + D_{p\rho} \frac{\partial g}{\partial p} \right].$$
(93)

We note that Equations (91) and (93) are exact.

A.1. Diffusion Approximation

We approximate the anisotropy Equation (93) assuming small anisotropies, i.e.,

$$|g| \ll F. \tag{94}$$

We also assume that $D_{\mu p}$ and D_{pp} are about a factor ϵ and ϵ^2 , respectively, with $\epsilon = V_{\rm A}/v \simeq V_{\rm A}/c \ll 1$, smaller than $D_{\mu\mu}$. To leading order this provides for Equation (93)

$$v\mu \frac{\partial F}{\partial z} \simeq \frac{\partial}{\partial \mu} \left[D_{\mu\mu} \frac{\partial g}{\partial \mu} + D_{\mu p} \frac{\partial F}{\partial p} \right].$$
 (95)

The same approximation (94) applied to Equation (91) provides the steady-state diffusion-convection transport equation for the isotropic part of the cosmic ray phase space distribution as

$$\frac{v}{2} \frac{\partial}{\partial z} \int_{-1}^{1} d\mu \mu g + \mathcal{R}F - S(\mathbf{x}, p)$$

$$\simeq \frac{1}{2p^{2}} \frac{\partial}{\partial p} p^{2} \int_{-1}^{1} d\mu \left[D_{\mu p} \frac{\partial g}{\partial \mu} + D_{pp} \frac{\partial F}{\partial p} \right]. \tag{96}$$

A.2. Anisotropy

Integrating Equation (95) provides

$$D_{\mu\mu}\frac{\partial g}{\partial \mu} + D_{\mu\rho}\frac{\partial F}{\partial \rho} = c_0 + \frac{\Gamma \nu \mu^2}{2}\frac{\partial F}{\partial z}.$$
 (97)

The integration constant c_0 (with respect to μ) is determined from the property that the left-hand side of this equation vanishes for $\mu=\pm 1$, because of property (92), yielding

$$c_0 = -\frac{\Gamma v}{2} \frac{\partial F}{\partial z},\tag{98}$$

and thus for Equation (97)

$$\frac{\partial g}{\partial \mu} = -\frac{v(1-\mu^2)}{2D_{\mu\mu}(\mu)} \frac{\partial F}{\partial z} - \frac{D_{\mu p}(\mu)}{D_{\mu\mu}(\mu)} \frac{\partial F}{\partial p}.$$
 (99)

Integrating Equation (99) again over μ , we obtain

$$g(\mathbf{x}, p, \mu) = c_1 - \frac{v}{2} \frac{\partial F}{\partial z} \int_{-1}^{\mu} dy \, \frac{(1 - y^2)}{D_{\mu\mu}(y)} - \frac{\partial F}{\partial p} \int_{-1}^{\mu} dy \, \frac{D_{\mu p}(y)}{D_{\mu\mu}(y)}.$$
(100)

The second integration constant c_1 (with respect to μ) is determined from condition (6). Using the integral for any function $h(\mu)$ and general $n \ge 0$

$$\int_{-1}^{1} d\mu \mu^{n} \int_{-1}^{\mu} dy \, \frac{h(y)}{D_{\mu\mu}(y)}$$

$$= \frac{1}{n+1} \int_{-1}^{1} d\mu \, \frac{(1-\mu^{n+1})h(\mu)}{D_{\mu\mu}(\mu)}$$
(101)

we find especially for n = 0

$$c_{1} = \frac{v}{4} \frac{\partial F}{\partial z} \int_{-1}^{1} d\mu \frac{(1-\mu)(1-\mu^{2})}{D_{\mu\mu}(\mu)} + \frac{1}{2} \frac{\partial F}{\partial p} \int_{-1}^{1} d\mu \frac{(1-\mu)D_{\mu\nu}(\mu)}{D_{\mu\nu}(\mu)}.$$
 (102)

This provides for the cosmic ray anisotropy (100)

$$g(\mathbf{x}, p, \mu) \simeq g_{s}(\mathbf{x}, p, \mu) + g_{c}(\mathbf{x}, p, \mu),$$

$$g_{s}(\mathbf{x}, p, \mu) = -\frac{v}{4} \frac{\partial F(\mathbf{x}, p)}{\partial z} \left[2 \int_{-1}^{\mu} dy \, \frac{1 - y^{2}}{D_{\mu\mu}(y)} \right]$$

$$- \int_{-1}^{1} d\mu \, \frac{(1 - \mu)(1 - \mu^{2})}{D_{\mu\mu}(\mu)} ,$$

$$g_{c}(\mathbf{x}, p, \mu) = -\frac{1}{2} \frac{\partial F(\mathbf{x}, p)}{\partial p} \left[2 \int_{-1}^{\mu} dy \, \frac{D_{\mu p}(y)}{D_{\mu\mu}(y)} \right]$$

$$- \int_{-1}^{1} d\mu \, \frac{(1 - \mu)D_{\mu p}(\mu)}{D_{\mu\mu}(\mu)} ,$$
(103)

which is the sum of the so-called streaming (g_s) and interstellar Compton–Getting (g_c) anisotropies, determined by the gradients of the isotropic distribution function F(x, p) with respect to z and p.

A.3. Anisotropy Moments

With the anisotropy Equations (99) and (103) we determine the moments needed in the diffusion-convection transport Equation (96). Using integral (101) for n = 1 we find

$$\int_{-1}^{1} d\mu \mu g = -\frac{vK_0}{4} \frac{\partial F}{\partial z} - \frac{H_0}{2} \frac{\partial F}{\partial p}$$
 (104)

with

$$K_0 = \int_{-1}^1 d\mu \, \frac{(1 - \mu^2)^2}{D_{\mu\mu}(\mu)},$$

$$H_0 = \int_{-1}^1 d\mu \, \frac{(1 - \mu^2)D_{\mu\mu}(\mu)}{D_{\mu\mu}(\mu)}.$$
(105)

Likewise

$$\int_{-1}^{1} d\mu \, D_{\mu p} \frac{\partial g}{\partial \mu} = -\frac{\nu H_0}{2} \frac{\partial F}{\partial z} - \frac{\partial F}{\partial p} \int_{-1}^{1} d\mu \, \frac{D_{\mu p}^2(\mu)}{D_{\mu \mu}(\mu)}. \quad (106)$$

Inserting the moments (104)–(106) in Equation (96) provides the steady-state diffusion-convection transport Equation (8) given above.

ORCID iDs

R. Schlickeiser https://orcid.org/0000-0003-3171-5079 M. Zhang https://orcid.org/0000-0003-3529-8743

References

```
Abramowitz, M., & Stegun, I. A. 1972, Handbook of Mathematical Functions
  (New York: Dover)
Ahlers, M., & Mertsch, P. 2017, PrPNP, 94, 184
Amenomori, M., Ayabe, S., Bi, X. J., et al. 2006, Sci, 314, 439
Bell, A. R. 1978, MNRAS, 182, 147
Blies, P., & Schlickeiser, R. 2012, ApJ, 751, 71
Casanova, S., & Schlickeiser, R. 2012, ApJ, 745, 153
Dung, R., & Schlickeiser, R. 1990a, A&A, 237, 504
Dung, R., & Schlickeiser, R. 1990b, A&A, 240, 537
Earl, J. A. 1974, ApJ, 193, 231
Erlykin, A. D., Machavariani, S. K., & Wolfendale, A. W. 2019, AdSpR,
Erlykin, A. D., & Wolfendale, A. W. 1997, JPhG, 23, 979
Hasselmann, K., & Wibberenz, G. 1968, ZGeo, 34, 353
Jokipii, J. R. 1966, ApJ, 146, 480
Ko, C.-M. 1992, A&A, 259, 377
Mertsch, P., & Funk, S. 2015, PRL, 114, 021101
Schlickeiser, R. 1989, ApJ, 336, 243
Schlickeiser, R. 2002, Cosmic Ray Astrophysics (Berlin: Springer)
Schlickeiser, R. 2011, ApJ, 732, 96
Schlickeiser, R., Caglar, M., & Lazarian, A. 2016, ApJ, 824, 89
Schlickeiser, R., & Shalchi, A. 2008, ApJ, 686, 291
Schlickeiser, R., Webber, W. R., & Kempf, A. 2014, ApJ, 787, 35
Shalchi, A. 2009, Nonlinear Cosmic Ray Diffusion Theories (Berlin: Springer)
Vainio, R., & Schlickeiser, R. 1998, A&A, 331, 793
Zhang, M., & Pogorelov, N. 2017, ICRC, 301, 502
Zhang, M., Zuo, P., & Pogorelov, N. 2014, ApJ, 790, 5
```